

UNCLASSIFIED

AD 404 920

DEFENSE DOCUMENTATION CENTER

FOR

SCIENTIFIC AND TECHNICAL INFORMATION

CAMERON STATION, ALEXANDRIA, VIRGINIA



UNCLASSIFIED

NOTICE: When government or other drawings, specifications or other data are used for any purpose other than in connection with a definitely related government procurement operation, the U. S. Government thereby incurs no responsibility, nor any obligation whatsoever; and the fact that the Government may have formulated, furnished, or in any way supplied the said drawings, specifications, or other data is not to be regarded by implication or otherwise as in any manner licensing the holder or any other person or corporation, or conveying any rights or permission to manufacture, use or sell any patented invention that may in any way be related thereto.

CATALOGED BY ASI/A
AD No. 404 920

6335

MONITORING AGENCY NO: ARL 62-460

ASTIA DOCUMENT NO:

CONTRACT AF 61 () -

TECHNICAL FINAL REPORT

Development of Methods for Quantitative
Spectroscopic Temperature Determination
of Plasmas

by

Dr. Hans Jürgen Kusch

Institute of Experimental Physics

University of Kiel, Germany

June 30, 1962

" This report was supported in whole or in part by
Plasma Physics Research Branch of the Aeronautical
Research Laboratories (ARL) , Office of Aerospace
Research (OAR) , UNITED STATES AIR FORCE, through
its European Office under Grant No. AF-EOARDC 61-29 "

404 920

MONITORING AGENCY NO:

ASTIA DOCUMENT NO:

CONTRACT AF 61 () -

TECHNICAL FINAL REPORT

Development of Methods for Quantitative
Spectroscopic Temperature Determination
of Plasmas

by

Dr. Hans Jürgen Kusch

Institute of Experimental Physics

University of Kiel, Germany

June 30, 1962

" This report was supported in whole or in part by
Plasma Physics Research Branch of the Aeronautical
Research Laboratories (ARL) , Office of Aerospace
Research (OAR) , UNITED STATES AIR FORCE, through
its European Office under Grant No. AF-EOARDC 61-29 "

Abstract.

During the last two years at Kiel institute three ways have been followed to obtain plasmas with temperatures up to $100\,000^{\circ}\text{K}$. The first approach pulsing an arc by high current was not as successful as desired because confinement breaks down. The second experiment was a linear pinch. In the center of the discharge temperatures higher than $80\,000^{\circ}\text{K}$ could be measured the radiation being emitted from thermally excited atoms.

The third way this report deals with is the magnetic compression of a preionized discharge in helium by an outer magnetic field. Preionization was effected by use of a pulsed discharge fed by a capacitor bank. Plasma parameters were determined using quantitative spectroscopic methods. Distributions of plasma parameters in space and time could be investigated by time resolved spectroscopy. Electron density rises to more than 10^{18} cm^{-3} ; temperature was found to be $70\,000^{\circ}\text{K}$ at most. Several methods to determine plasma parameters yielded the same results thus proving the plasma to be in local thermodynamic equilibrium. Radiation was found to be emitted from optically thin layers.

With more energy stored in the capacitor bank feeding the magnetic field and a still more effective preionization a further increase in temperature may be expected.

Table of contents

Page	
3	A. Introduction
4	B. The experimental set up
4	1a) Circuit for the production of the quickly rising magnetic field
9	1b) The operation of the trigger circuit
10	1c) The preionization
12	1d) The glow discharge
12	2) The discharge tube
14	3) The optical arrangement and the photographic technique
18	C. Spectroscopic theory
18	1) The composition of the plasma
19	2) Line intensities
19	3) The continuous emission
21	4) Line broadening
21	D. Results
21	1) The preionization
23	2) The magnetic compression
25	2a) The evaluation of the spectra
25	α) Temperature measurement from the relative intensities of two lines of different ionization stages
25	β) Temperature measurements from absolute continuum intensity

Page

28	γ) Temperature determination from the intensities of a neutral line and the continuum
28	δ) Temperature determination from neutral line intensity
28	2b) Plasma data in the magnetic compression experiment
33	E. Conclusion
34	Bibliography
35	Glossary of symbols
36	List of illustrations

A. Introduction

The interpretation of observations in astrophysics and of measurements in the field of thermonuclear fusion research is strongly dependent on the knowledge of properties of matter at very high temperatures. The most important parameters in a plasma are electron density, temperature of the several species of particles, and the composition of the plasma. In high-temperature plasmas these parameters can be obtained best by using quantitative spectroscopic methods. This procedure involves a complete understanding of line shifts and broadening and of line- and continuum intensities either from theory or from experimental investigation. In case of local thermodynamic equilibrium intensities and number densities of the components can be computed easily: at constant pressure these values are functions of temperature only, and this temperature is equal for all components. Because the width of spectral lines increases with rising electron density, isolated lines can only be observed at electron densities below an upper limit. On the other hand the configuration and the confinement of the plasma should be of simple geometry in order to allow an evaluation of temperature gradients and of the optical path.

Temperatures up to 20000°K ¹⁾, in exceptional cases up to 50000°K ²⁾, can be produced in stationary arc discharges. A further rise in temperature is limited by the wall materials' breaking down. It appears possible to investigate temperature rises during a short interval of time in pulsed arc discharges ³⁾. But in this kind of discharges pressure is unknown; in addition fluctuations and oscillations of the plasma influence severely a detailed investigation.

Another method to produce plasmas in the range of 20000° to 100000°K is to compress and so to heat a plasma by means of magnetic fields; to approaches were made in this field of research: the linear pinch ⁴⁾ and the compression of a plasma by an external magnetic field (or θ -pinch) ⁵⁾.

In this report we will deal with the quick magnetic compression of a preionized helium plasma. Helium has been chosen, because oscillator strengths, continuum absorption coefficients, and line broadening parameters are well known for this element.

B. The Experimental Set up.

1a) Circuit for the production of the quickly rising magnetic field.

Twenty capacitors $40 \mu\text{F}$, 6 kV each are connected by a linear transmission line of low inductivity as shown in fig. 1, allowing a loading voltage of 12 kV. The transmission line consists

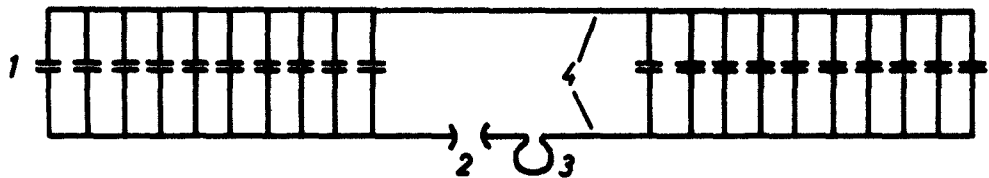


Fig. 1. The connection of the capacitors (schematic).

1. capacitors $40 \mu\text{F}$, 6 kV
2. spark gap
3. coil
4. transmission line

of flat parallel leads of aluminum 1 cm thick and 20 cm broad each, and of a thin copper sheet being the other conductor. The two leads and the copper conductor are separated by 0.5 mm Hostaphan (or Mylar) with a break down potential of 160 kV/mm, and pressed together by clamps. The capacitors are fixed to the leads by coaxial connectors. A cross section of the complete line is shown in fig. 2.

The discharge circuit was operated by a spark gap triggered

externally, thus producing the magnetic field in a one turn coil.

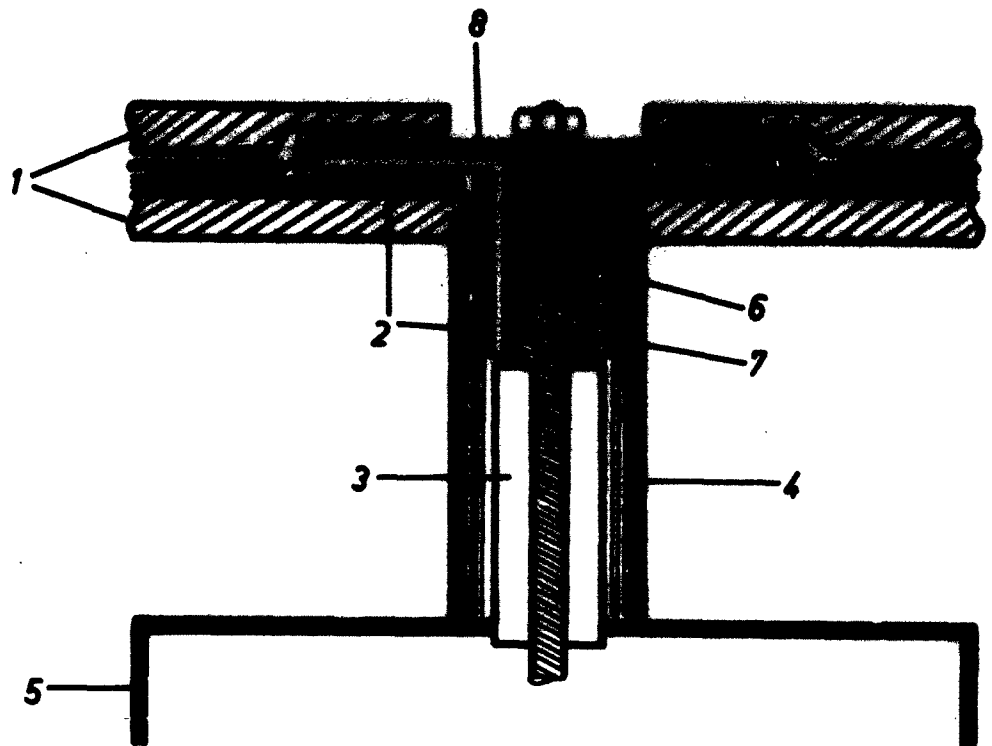


Fig. 2. Connection of the capacitors to the linear transmission line.

1. parallel leads of aluminum 1 cm thick 20 cm broad each
2. Hostaphan insulation
3. ceramic insulator fastened to the condensor casing 5
4. outer conductor of the coaxial lead
6. rubber insulator
7. inner conductor of the coaxial lead
8. copper sheat 0.5 mm thick

The coil of iron, inner diameter 4.5 cm and 8.0 cm long, is welded carefully to an iron part of the transmission line smoothly enlarging to a width of 20 cm. Because of skin effect the current passes only at the inner surface of the coil; therefore the outer form of the coil is practically without influence. On one side the iron part is screwed firmly to the aluminum lead using soft

copper to reduce electrical resistance. On the other side the coil is connected to the sparc gap switch of small inductivity, intersecting the transmission line. The sparc gap made out of iron is shown in fig. 3. One rod of the gap is fitted with 5 trigger pins; the 5 triggering sparks are fired simultaneously in parallel in order to reduce the inductivity of the gap to one fifth of the inductivity of a single sparc. A view of the entire installation can be seen from the photograph, fig. 4.

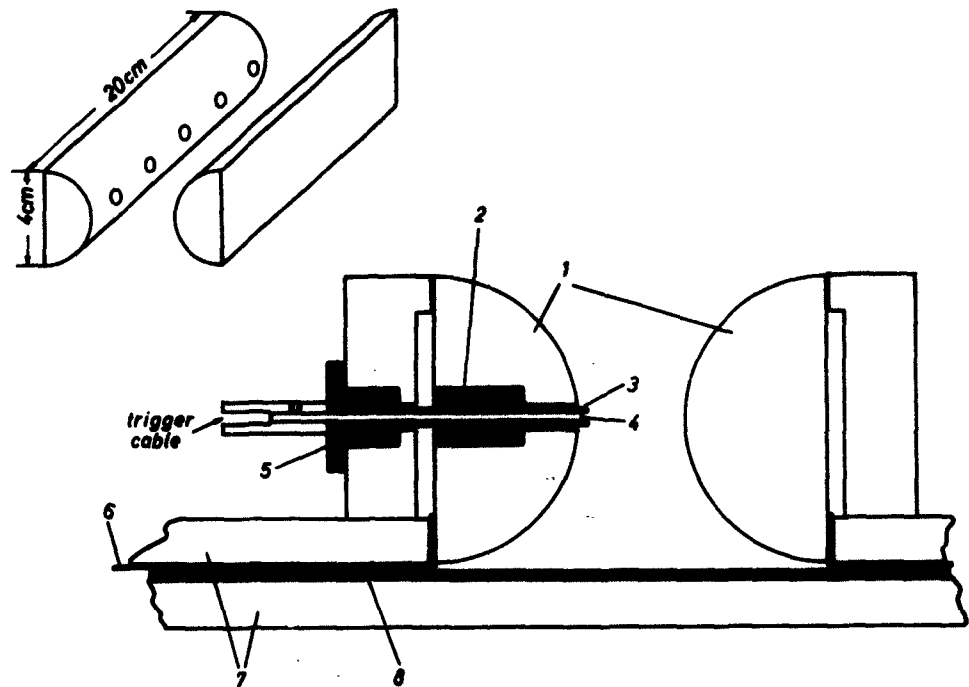


Fig. 3. Sparc gap of half-cylindrical shape.

1. iron electrodes 20 cm broad each
2. talc insulation
3. insulating tubing made out of plastic
4. trigger rod (steel)
5. insulator made out of Pertinax
6. copper sheat, see fig. 2
7. leads of aluminum
8. Hostaphan insulation

Using a small probing coil, the time of one oscillation of the total installation was measured to be $\tau = 22.0 \mu\text{sec}$,

corresponding to a frequency of 45.5 kcycles/sec.

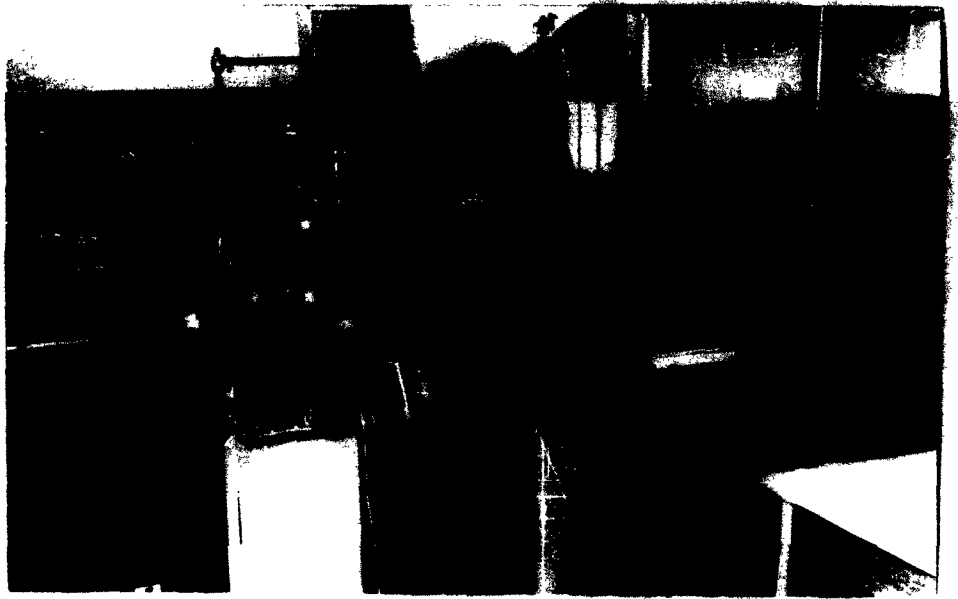


Fig. 4. Total view of the pulse current condenser bank (viewed from the side). Notice spark gap and one turn coil, and at left hand of the picture 12 kV voltage supply and triggering condenser.

From Thomson's formula for a damped oscillation:

$$\beta = 2\pi\sqrt{LC} \cdot \sqrt{1 + \frac{\Lambda^2}{4\pi^2}}$$

with Λ logarithmic decrementum, the total inductivity of the circuit can be obtained. With $\Lambda = 0.947$ we find:

$$L = 59.8 \text{ nHy.}$$

The capacitors were charged to $U_0 = 12 \text{ kV}$; so we obtained the current rise at $t = 0$

$$j| = \frac{U_0}{L} = 2.0 \cdot 10^{11} \text{ amps/sec.}$$

The maximum of the discharge current is calculated to be:

$$J_{\max} = U_0 \sqrt{\frac{C}{L}} = 6.58 \cdot 10^5 \text{ amps.}$$

The magnetic field H in the coil can be measured by a small probing coil the area of which is to be determined at first. This

was done by a high-frequency fed Helmholtz coil.

From Faraday's law we get the induced voltage:

$$V = - \frac{a}{c} \cdot \dot{H} \quad \text{or} \quad H(t) = - \frac{c}{a} \int_0^t V dt .$$

The probing coil was connected to a 60Ω -cable with a 60Ω resistor at the input of the oscilloscope. The voltage at time $t = 0$ could not be marked on the oscillograms inspite of carefully screening the coil by copper covering. Therefore the maximum voltage was extrapolated from the succeeding damped oscillations. In the maximum of the first half-period of the oscillation the magnetic field in the center of the coil was found to be

$$H = 98600 \text{ Oe}$$

at a charge potential of 12 kV. Mounting the coil at different radii the radial distribution of the magnetic field could be obtained. For the maximum of the second half-period this is shown in fig. 5.

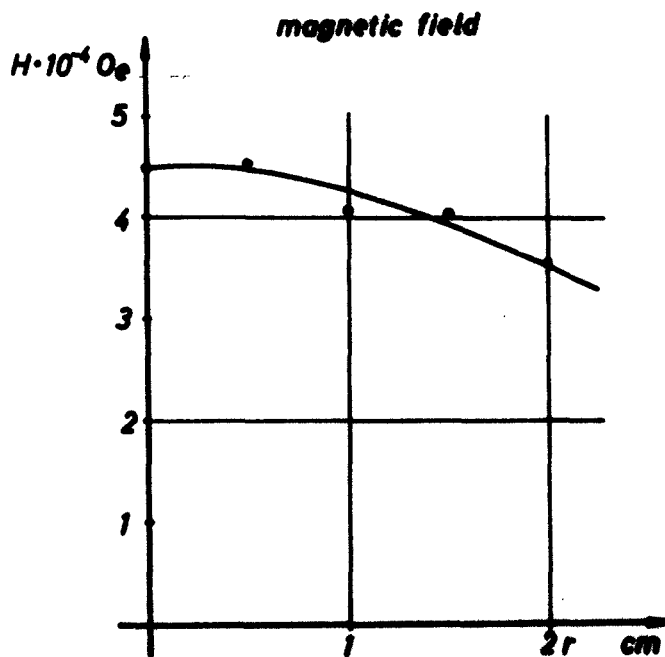


Fig. 5. Radial distribution of the magnetic field inside the coil, obtained in the second half-period of the magnetic field discharge using a small probing coil.

1b) The operation of the trigger circuit.

We explain the function of the circuit by considering fig. 6 and 7. A positive pulse of 200 V amplitude is given to the grid of a hydrogen thyatron PL 435. This getting conductive a capacitor of $0.1 \mu\text{F}$ previously charged to 12 kV causes a potential drop at the resistor $25 \text{ k}\Omega$ thus firing the sparc gap 1. The 12 kV-pulse produced here results nearly simultaneously into firing the five sparc at the end of the parallel coaxial cables.

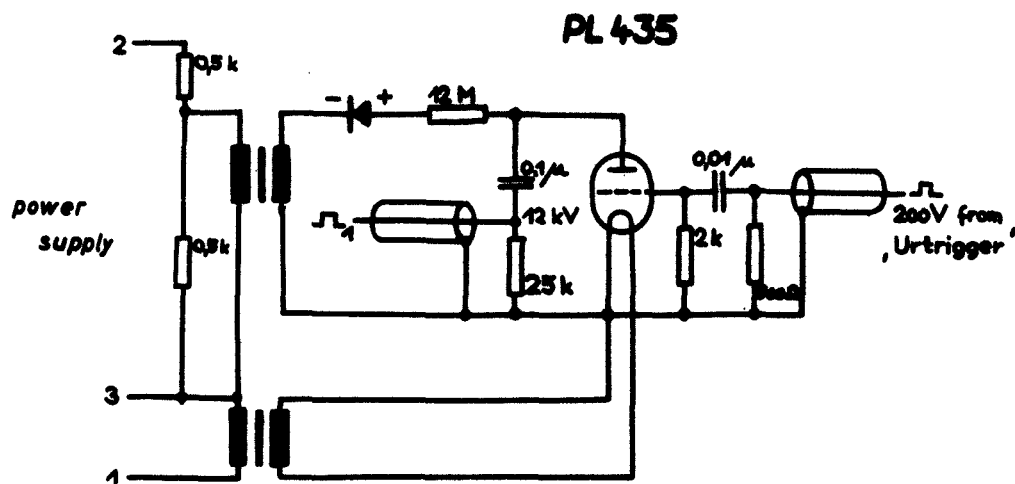


Fig. 6. Wiring of the triggering device switching the sparc gap.

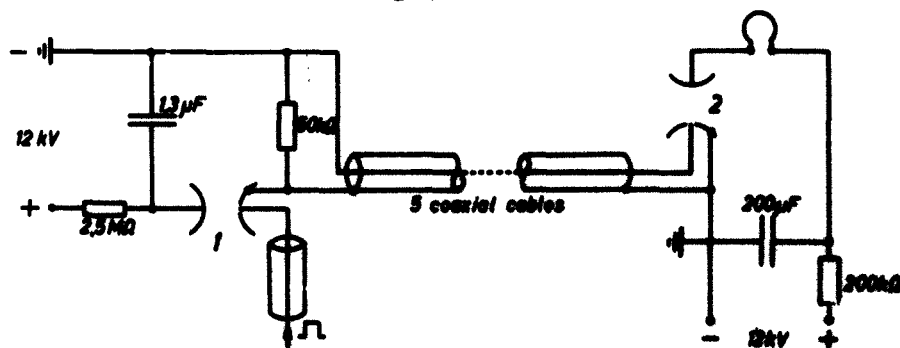


Fig. 7. Diagram of the trigger circuit.

lc) The preionization .

The effect of magnetic compression is strongly influenced by the efficiency of preionization. Earlier experiments taking a glow discharge only, were of small success because ionization was unsufficient. Using a capacitor bank as preionizing power supply the electron density and the electric conductivity of the helium plasma could be increased to a much larger scale. In order to obtain stationary conditions before and after magnetic compression the battery was connected to give a rectangular current pulse during ca. 500 μ sec. This could be done using resistors and coils as additional elements. The coils were wound on insulating tubes and then fixed with shellac, to sustain the magnetic forces. The preionizing circuit is shown in fig. 8. The current pulse can be seen from fig. 9.

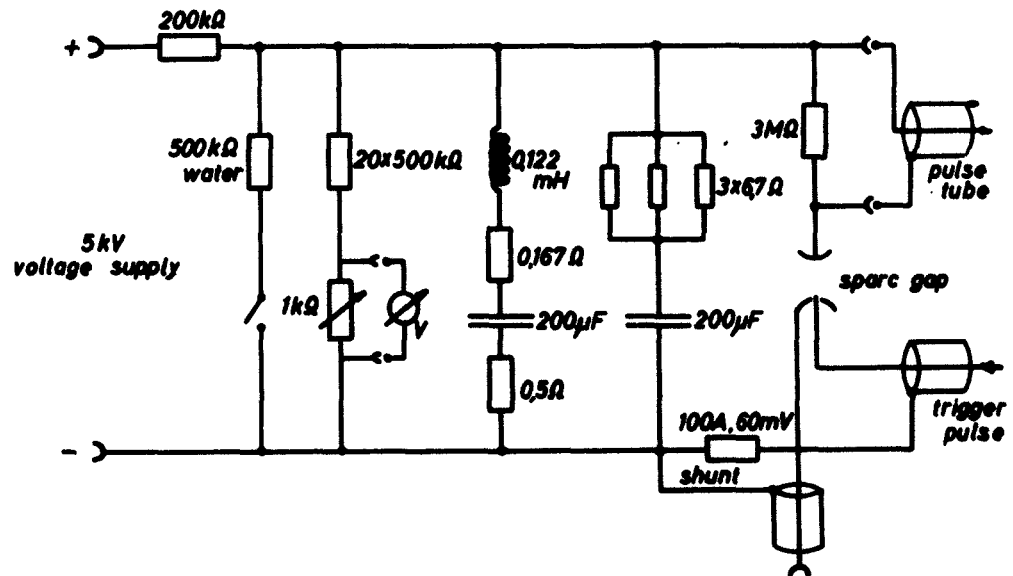


Fig. 8. Wiring of the capacitor bank used for preionization.

The capacitor bank could be fired by a sparc gap of half-spherical shape using the triggering device of fig. 10 which was started with a light pulse.

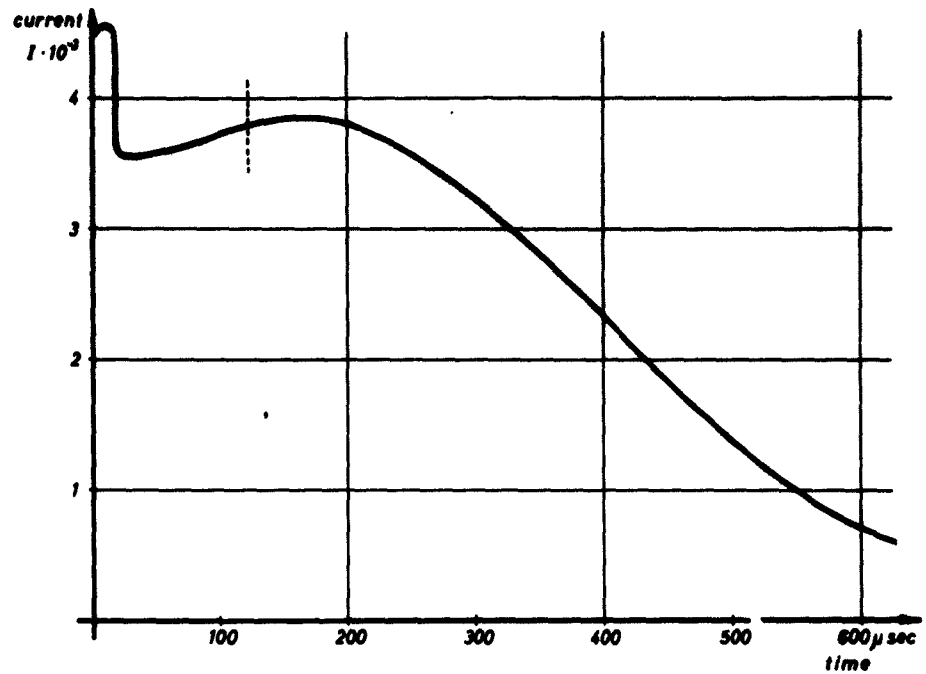


Fig. 9. Current of preionizing discharge. The dotted line denotes the time where the magnetic field for compression is fired.

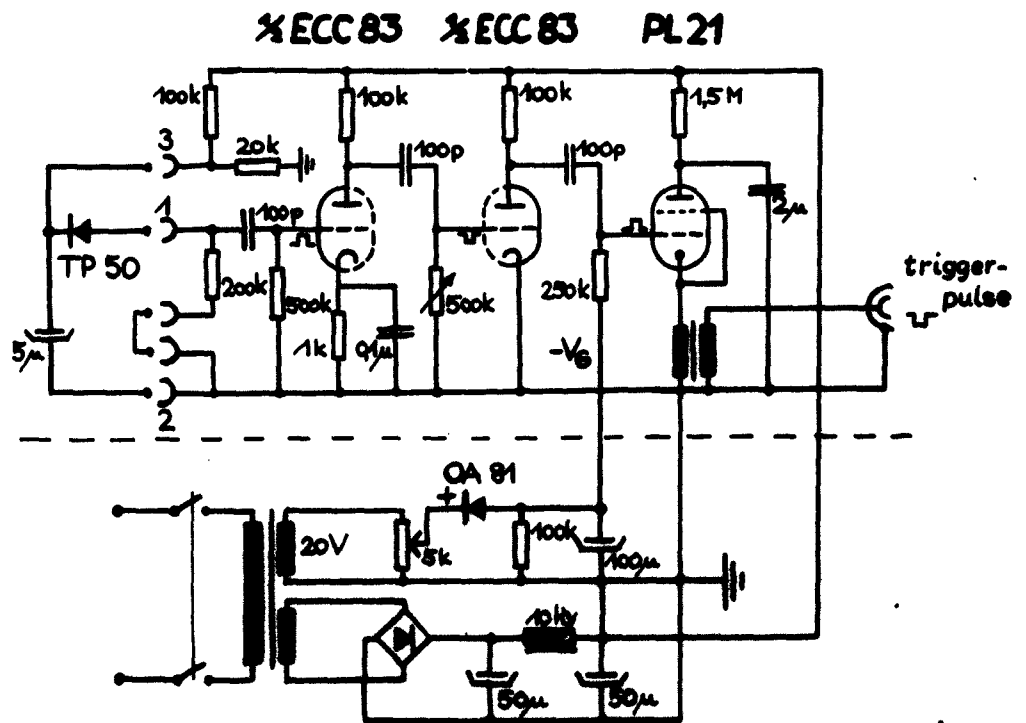


Fig. 10. Photodiode triggering device. Photodiode TP 50.

ld) The glow discharge.

Discharging a high current pulse through a tube of relatively large diameter the uniformity of the plasma is often disturbed by accidental effects at the electrodes or the surface of the tube. In order to avoid this and so to induce homogenous ionization, a glow discharge of 100 m amps was started before firing the capacitor bank. The high-voltage supply can be seen from fig. 11. In order not to destroy the device when firing the pulse, the discharge tube is separated from the high-voltage supply by a vacuum-tube rectifier AG 1006.

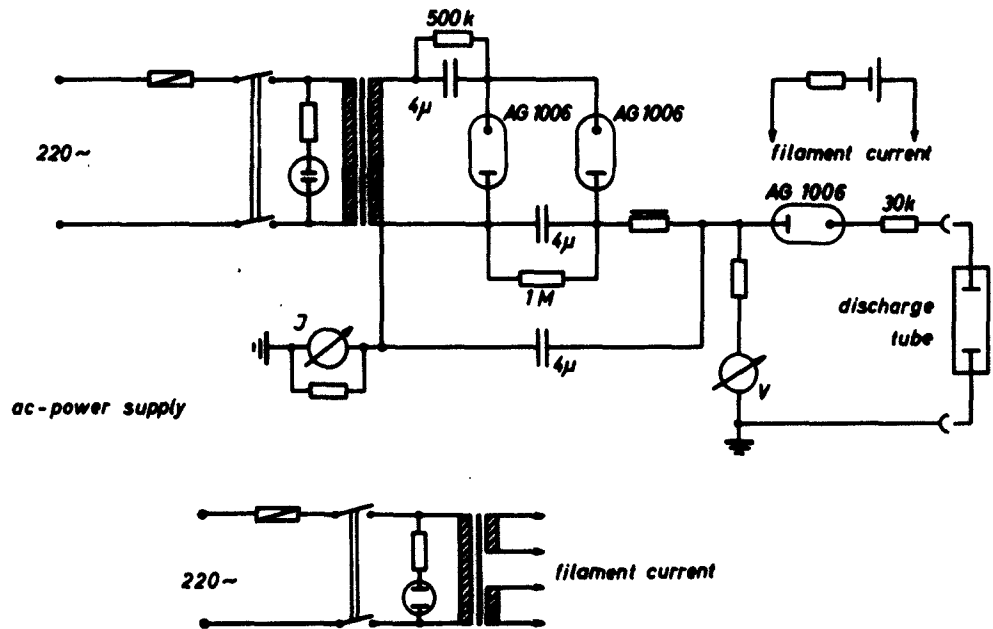


Fig. 11. Wiring of the high-voltage supply for the preionizing glow discharge.

2) The discharge tube.

The construction of the discharge tube is shown in fig. 12. Two electrodes of pure aluminum shaped as a half sphere and a plane respectively are fixed vacuumtight to a straight pyrex glass tube of 3.8 cm inner diameter and 13 cm height using plane

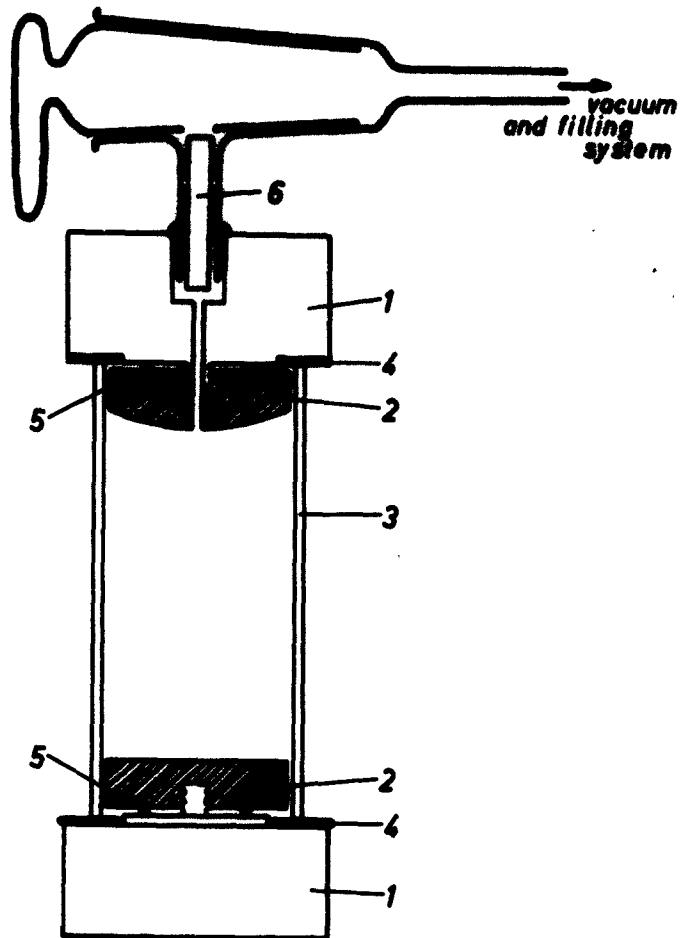


Fig. 12. Cross cut of the discharge tube.

1. Blocks of aluminum covering the ends of the discharge tube
2. electrodes made out of aluminum of high purity
3. pyrex glass tube
4. plane rubber rings
5. copper rings to reduce contact resistance
6. glass rod to keep the volume not heated small

rubber rings and clamps. The tube is mounted inside the coil and connected to the capacitor bank by a coaxial cable. To get a symmetrical discharge the backlead near the tube was made as cylindrical as possible using a number of copper wires of

suitable profile. After a careful evacuation to some 10^{-5} torr by a mercury diffusion pump system and cold traps the discharge tube was filled with commercial pure helium gas up to 12 torr pressure.

3) The optical arrangement and the photographic technique.

In order to obtain plasma parameters as a function of space and time the discharge was observed from the side through a slot in the coil of 2 mm width, arranged perpendicular to the axis of the discharge. So the radial distribution could be derived from the spectra using Abel's integral equation ⁶⁾.

We explain the operation of the optical arrangement using fig. 13. The light emitted from the plasma's cross section is

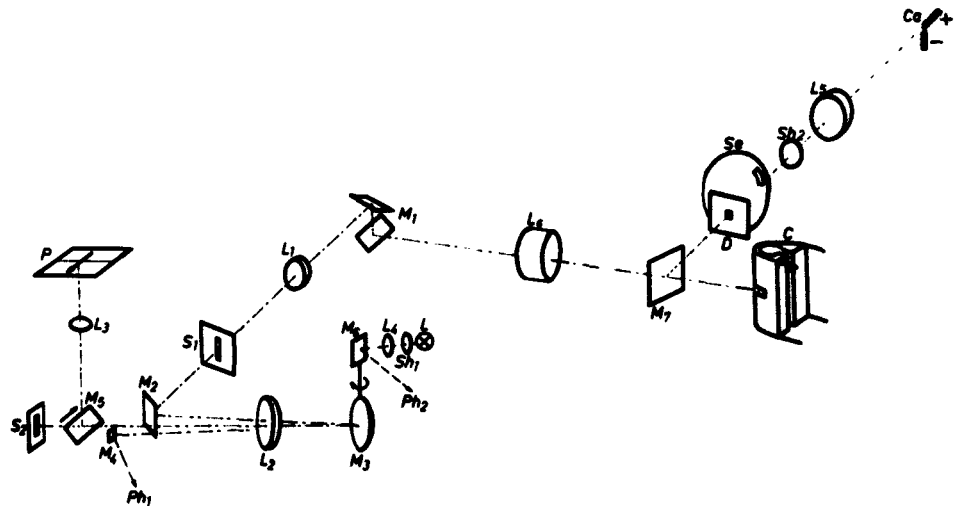


Fig. 13. Optical arrangement for time resolved spectroscopy of the pulsed discharge compressed by a quickly rising magnetic field. Ph₂ photodiode in fig. 10. Ph₁ photomultiplier device.

imaged to an auxiliary slit S₁ by the objective lenses L₁ and L₆ and the mirror system M₁, the beam between the lenses being in parallel. Then the light is reflected to the side by the mirror M₂ and made parallel by the objective lens L₂, at last

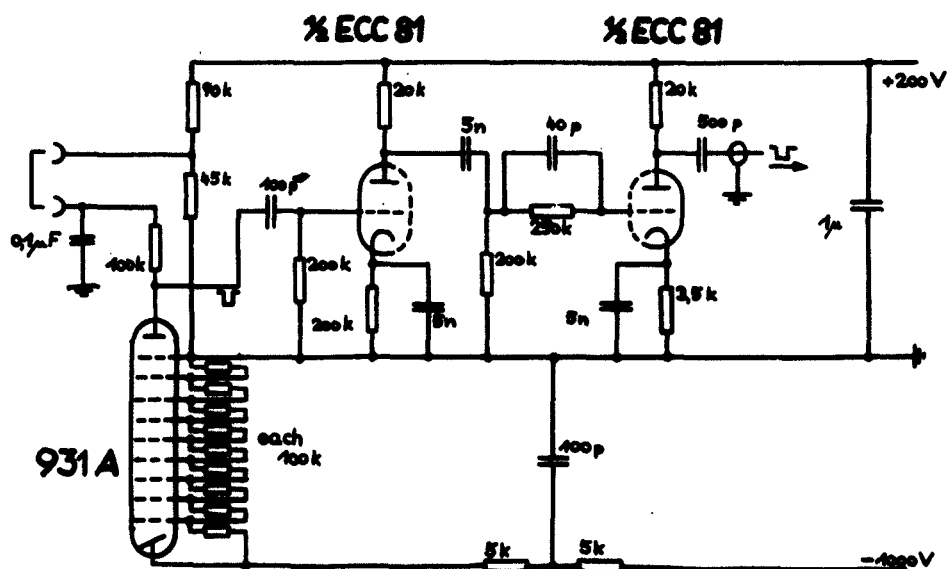


Fig. 14. Wiring of the photomultiplier triggering device.
 U is a negative pulse of 200 V.

The rotating mirror M_3 is a plane circular disk of 14 cm diameter made of silvered glass and spinning with a revolution

frequency ν of 175 rev/sec. With a slit width of S_1 $W=0.25$ mm, and the length of the light pointer $M_3L_2 = l = 30$ cm the time of exposure Δt is :

$$\Delta t = \frac{W}{4\pi l \nu} = 0.38 \text{ } \mu\text{sec} .$$

Special care was taken to intensity calibration and standardization of the photographic plates. Because of short exposure time effect and intermittancy effect calibration marks and the intensity normal have to be applied to the plate with about the same exposure time as the spectrum.

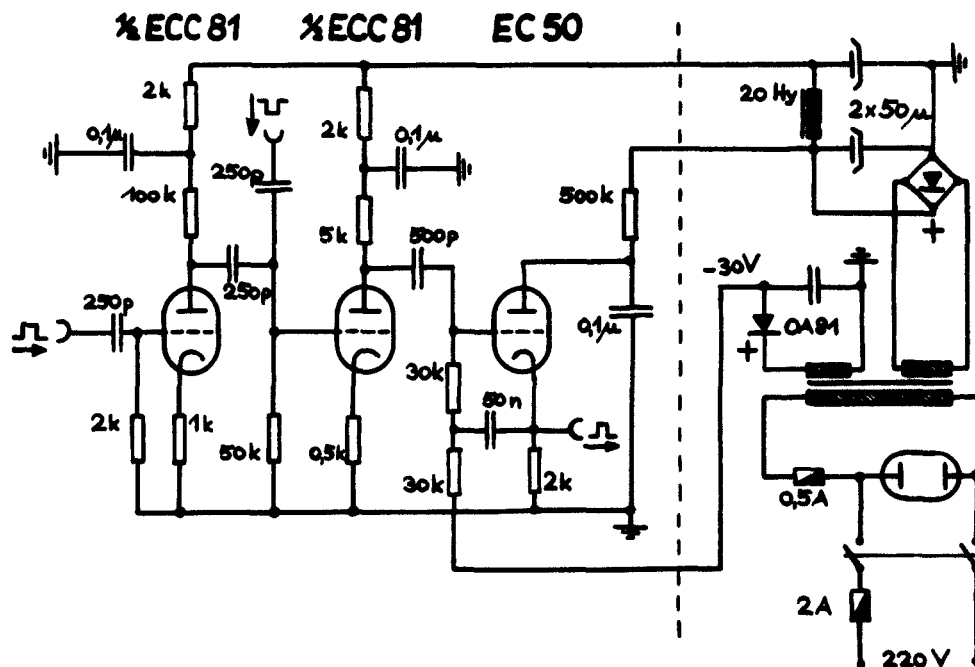


Fig. 15. Circuit of the "Urtrigger" mentioned in fig. 6.

The intensity standard was a carbon arc after Mc Pherson and Euler ⁷⁾, marked in fig. 13 by Ca. The anode of the arc is imaged to a diaphragm D of rectangular shape by the objective lens L_5 . An auxiliary mirror M_7 is put into the line of view making M_7D equal to the distance M_7 -center of the discharge tube. By a mechanical shutter Sh_2 and a rotating sector Se the light beam

is set free for one revolution of the mirror M_3 only to prevent double exposure. This was controlled by photoelectric means. Opening of the slit S_2 to a width four times larger than was used to obtain the spectrum of the discharge and taking a much larger solid angle (by moving away a diaphragm in front of L_6) allowed to obtain sufficient blackening of the plate by the intensity standard. The small change in exposure time resulting from opening the slit was taken into account by measuring the light pulses photoelectrically. The plate was standardized using either one or several pulses from the carbon arc; in the latter case the intensity was extrapolated from the function $I=f(n,\Delta t)$, where n is the number of exposures, as was furnished in a separate investigation.

Intensity calibration marks were taken using a luminous sparc of less than one μsec duration and taking care for uniform illumination of the slit of the spectrograph, which was covered with a platinum step reducer of known transparency.

The spectrograph used in this investigation was a three-prism-glass instrument after Försterling with a camera focal length of 27 cm and an aperture of 1:4.5. At 5800 \AA the linear dispersion was 97 \AA/mm and at 4400 \AA 29 \AA/mm . For exposure of the discharge the slit width was taken to be 0.09 mm; for standardization 0.36 mm. For the spectrum as well as for the smear camera Ilford HPS-plates were used and developed in Faber Strobfin for 25 minutes at 26° C .

The spectra of the preionizing discharge were taken without resolution in time. The effective time of exposure was determined to be 300 μsec by photoelectric measurement. The carbon arc was exposed for the same time using the rotating sector and shutter only, see fig. 13. Intensity marks were taken with step reducer, carbon arc and a rotating mirror system. The plates used were Pancola 17⁰ developed in Agfa Rodinal.

The obtained spectra were analysed using a microphotometer and a recorder of the type Rohde und Schwarz Enograph.

C. Spectroscopic Theory.

In this chapter a survey is given of the theoretical formulae used in spectroscopic plasma research. Determining plasma parameters one makes use of equations for line and continuum intensities and on the other hand Saha equations for the plasma's composition. These formulae are based on the assumption of local thermodynamic equilibrium. The intensities given in this chapter refer to optically thin layers.

1) The composition of the plasma.

Assuming the plasma is an ideal gas in local thermodynamic equilibrium, the populations of the different stages can be obtained from Saha's equation:

$$(1) \quad \frac{N_{r+1} N_e}{N_r} = 2 \frac{Z_{r+1}}{Z_r} \frac{(2\pi m_e kT)^{3/2}}{h^3} e^{-\frac{\chi_r - \Delta\chi}{kT}},$$

where the subscript r stands for the stage of ionization ($r=0$ neutral atom, $r=1$ single ionized, $r=2$ doubly ionized). χ_r are the ionization potentials respectively and Z_r the partition functions of species r ; N_e denotes the electron density. $\Delta\chi$ is the lowering of the ionization potential which was estimated as a function of electron density after Unsöld⁸⁾:

$$(2) \quad \Delta\chi = 2 \left(\frac{4\pi}{3} \right)^{1/3} e^2 N_e^{1/3}.$$

Furthermore is after Dalton's law:

$$(3) \quad N_e + \sum_{r=0}^2 N_r = \frac{p}{kT},$$

where p is the total pressure of the plasma.
Involving the quasi-neutrality condition:

$$(4) \quad N_e = \sum_{r=0}^2 (r-1) N_r$$

(1), (3), (4) mount into four equations determining the population

N_0 , N_1 , N_2 , and N_e as a function of p and T . The components of the plasma were computed by an electronic computer IBM 704 at several values of p and then plotted.

2) Line intensities.

The intensity of spectral line arising from a transition $m \rightarrow n$ is given by

$$(5) \quad I_{nm,r} = \frac{1}{4\pi} h \nu_{nm,r} A_{nm,r} N_{m,r} \cdot l$$

if one assumes optically thin layers.

In this formula are:

- $\nu_{nm,r}$ the frequency of the line $m \rightarrow n$ of species r
- $A_{nm,r}$ the transition probability
- $N_{m,r}$ the population of the upper level m of species r
- l the length of the emitting layer.

In case of local thermodynamic equilibrium the concentration of atoms is given by

$$(6) \quad N_{m,r} = N_r \frac{g_{m,r}}{Z_r} e^{-\frac{\chi_{m,r}}{kT}},$$

where $g_{m,r}$ is the statistical weight of the upper state and $\chi_{m,r}$ its excitation potential.

3) The continuous emission.

The continuum emitted from high-temperature helium plasmas consists of three components, the free-bound transitions of neutral and ionized helium and the free-free transitions. The continuous absorption coefficients can be calculated in the hydrogenic approximation, the so called Unsöld formula ⁹⁾. Per hydrogen atom the total absorption coefficient is:

$$(7) \quad \kappa_\nu = \frac{64\pi^4}{3\sqrt{3}} \frac{m_e e^{10} Z^4}{c h^6} \frac{1}{\nu^3} \frac{e^{-u_1}}{2u_1} \left\{ e^{u_{n+1}} + 2u_1 \sum_{u_n < \frac{h\nu}{kT}} \frac{e^{u_n}}{n^3} \right\}$$

with $u_n = \frac{RhcZ^2}{n^2 kT}$.

Applying this formula to neutral helium it should be corrected by a factor of 2 because in this case there is a singlet and a triplet system. The continuum of the hydrogenic helium ion can be calculated from the above formula without any alteration.

The free-free continuous emission can be calculated using Kramers' formula ¹⁰⁾:

$$(8) \quad \kappa_v^{ff} = \frac{4\sqrt{2\pi} e^6 Z^2}{3\sqrt{3} h m_e^2 c h \nu^3 \sqrt{T}}$$

Including induced emission we finally obtain the continuous intensity:

$$(9) \quad I_{cont, \nu} = B_\nu \left(1 - e^{-\frac{h\nu}{kT}}\right) \left\{ \kappa_v^{H_2} N_0 + \kappa_v^{H_2^+} N_1 + \kappa_v^{ff} N_0 N_1 \right\}.$$

These intensities were calculated with the plasma composition in part 1) and then plotted as a function of T for several values of p, see fig. 16.

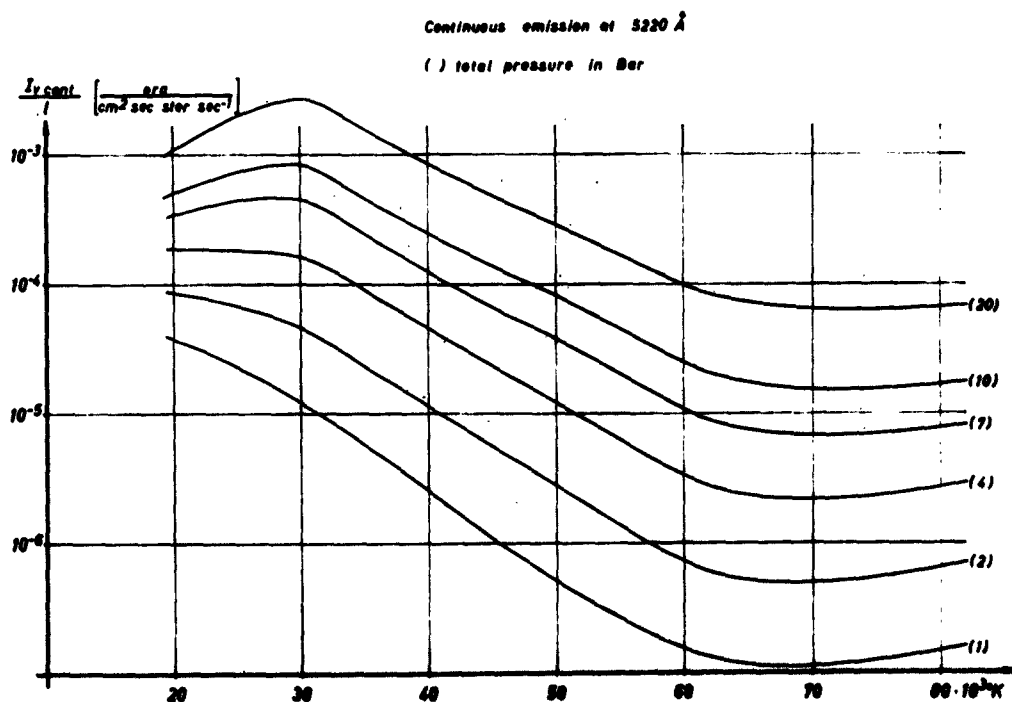


Fig. 16. The continuous emission of a helium plasma at 5220 Å.

4) Line broadening.

The half width of helium lines neutral as well as ionized is obtained from the recent theoretical works of Griem, Baranger, Kolb and Oertel ¹¹⁾ and Shen ¹²⁾ or from Berg's experimental values ¹³⁾.

D. Results.

The obtained spectra were analysed using Abel's integral equation:

$$I(x) = 2 \int_x^{r_0} \frac{i(r) r dr}{\sqrt{r^2 - x^2}}$$

with the preassumption of rotational symmetry in the plasma. The equation was solved using a set of coefficients computed by Sörensen and Richter ¹⁴⁾. This yields the spectral intensity $i(r)$ and therewith the radial distribution of the plasma parameters.

1) The preionization.

The spectrum of the preionizing discharge consists of neutral helium lines only (see fig. 20). From the half width of the line $5876 \text{ \AA } 3^3D_3 - 2^3P_2^0$ or $4471 \text{ \AA } 4^3D_3 - 3^3P_2^0$ the electron density could be obtained. The radial distribution is shown in fig. 17. From the absolute intensities of 5876 \AA or of 4471 \AA (in the latter case neglecting the forbidden components) ^{+) temperature and pressure can be calculated using formula (5) in chapter C 2) and the plots of the plasma composition. The radial distributions of temperature and total pressure can be seen in fig. 18 and fig. 19.}

^{+) For the oscillator strengths see Allen ¹⁵⁾.}

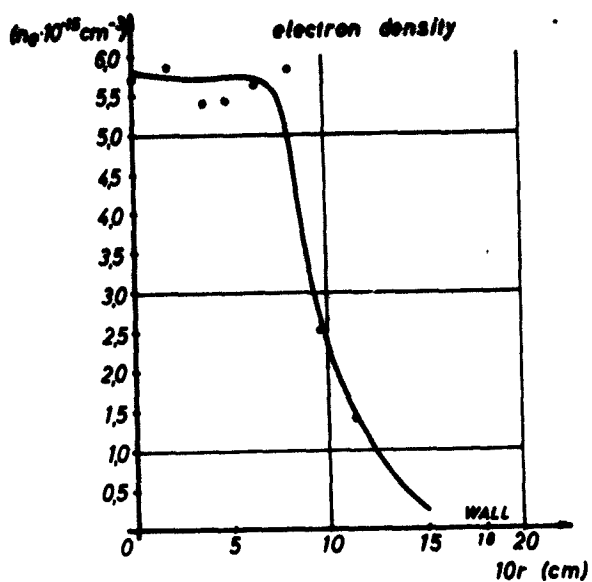


Fig. 17. The radial distribution of the electron density in the preionizing discharge.

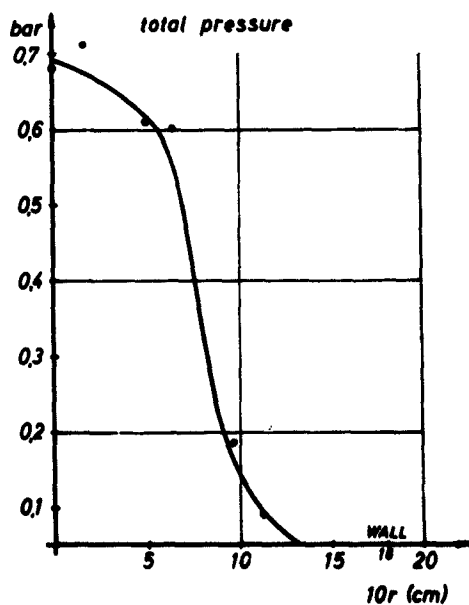


Fig. 18. The radial distribution of total pressure in the preionizing discharge.

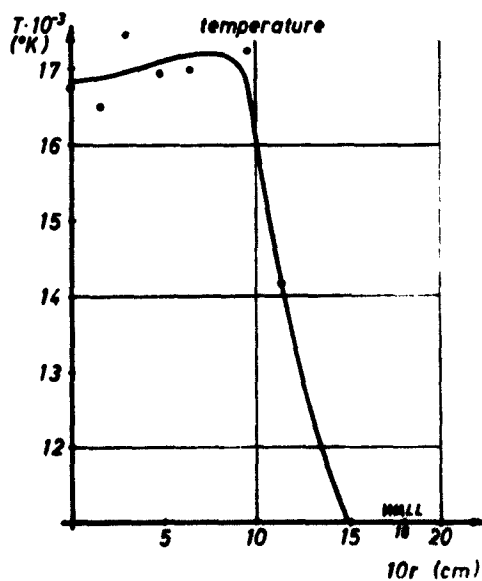


Fig. 19. The radial distribution of temperature in the preionizing discharge.

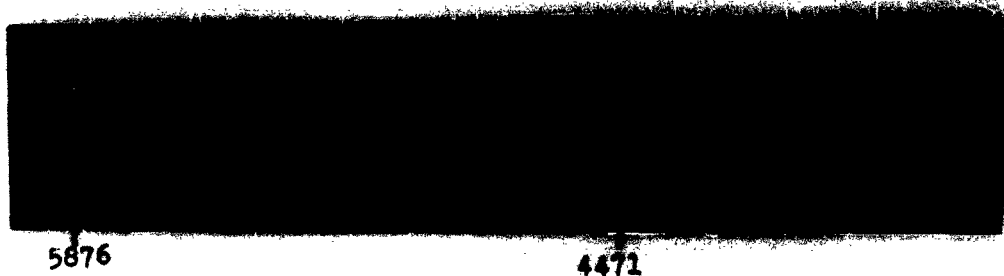


Fig. 20. The spectrum of the preionizing discharge. Notice only neutral helium lines are emitted. Initial pressure 12 torr helium. Slit width of the spectrograph 0.06 mm corresponding to 0.054 mm on the plate. Interval of exposure 300 μ sec.

2) The magnetic compression.

To give a general view of the phenomenon a smear photograph of the discharge is shown in fig. 21. The luminosity of the

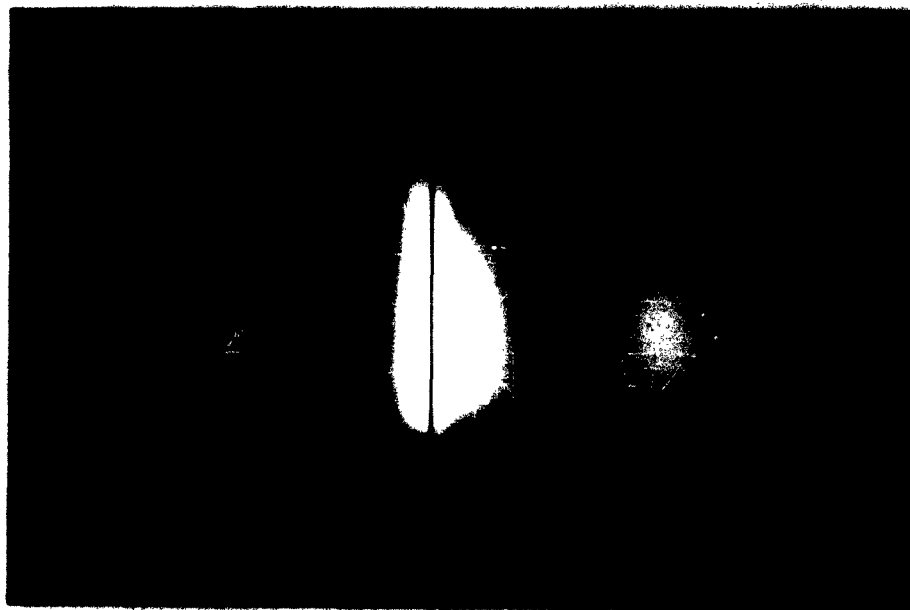


Fig. 21. Smear camera photograph of a pulsed helium discharge compressed by a quickly rising magnetic field. Initial pressure 12 torr helium. Loading voltage of the preionizing condensor bank: 4.2 kV loading voltage of the magnetic compression condensor bank 12.0 kV. Time resolution 1.986 mm/ μ sec. Scale of imaging: 1 cm in the discharge corresponds to 1.503 cm on the smear camera plate. Enlarged 1 : 1.92. For the arrow see fig. 30 and fig. 31.

plasma is strongly increased by the magnetic compression. The distribution in time of the light emission is synchronous to $H \cdot \dot{H}$ the interval between the several bounces being 6 μsec . At the time resolution used the preionizing discharge is too weak to effect blackening of the smear photographic plate. During the first half-period of the magnetic field oscillation the preionized plasma is heated further. A characteristic spectrum exposed in the first half-period is shown in fig. 22.

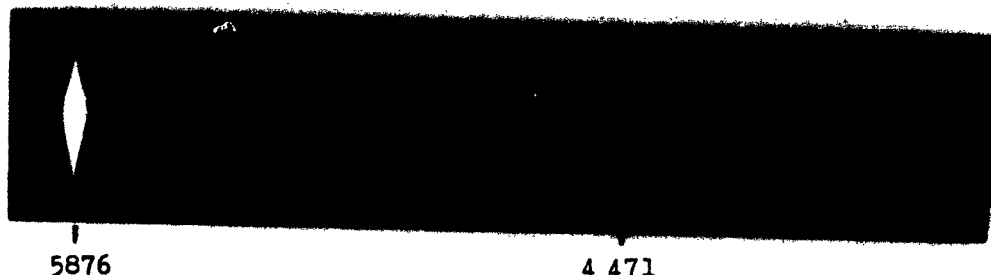


Fig. 22. Characteristic spectrum exposed in the first half-period of magnetic compression. Notice strongly broadened neutral helium lines and absence of any ionized lines. Interval of exposure 0.38 μsec .

In spite of relatively good preionization only much broadened lines of neutral helium are emitted from the discharge. As $H \cdot \dot{H}$ rises to its second half-period the plasma is heated more thus emitting the very intensive ionized helium line 4686 \AA , the neutral line 5876 \AA , and a luminous continuum background. A characteristic spectrum of this phase of the discharge is shown in fig. 23.

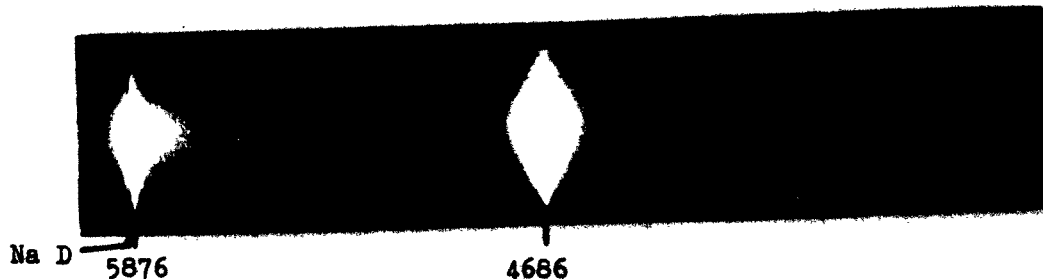


Fig. 23. Characteristic spectrum exposed in the second half-period of the magnetic compression. Interval of exposure 0.38 μsec .

2a) The evaluation of the spectra.

In this chapter firstly a survey is given of the different methods used to determine plasma parameters. The electron density is obtained always from line broadening. For the different lines plots have been made of the half widths versus N_e . At high temperature the electron density was obtained from the width of He II 4686 Å; at lower temperatures where no He II lines occur He I 5876 Å or He I 4471 Å was used. We firstly describe the methods of temperature determination at high temperatures (more than about 35000° K).

α) Temperature measurement from the relative intensities of two lines of different ionization stages.

Using equations (5) and (6) the intensity ratio of a He II line and a He I line $\frac{I_2}{I_1}$ can be written:

$$(10) \quad \frac{I_2}{I_1} = \frac{v_2 A_2 \cdot N_2(p, T)}{v_1 A_1 \cdot N_1(p, T)},$$

where $\frac{N_2}{N_1}$ is the ratio of the populations of the upper states. The ratio $\frac{N_2}{N_1}$ as a function of temperature and pressure is plotted in fig. 24. The population of the upper state of the line 4686 Å is shown in fig. 25. With the electron density from line broadening temperature and total pressure can be obtained from the plot.

β) Temperature measurement from absolute continuum intensity.

From equation (9) or from fig. 16 the absolute continuous emission is obtained as a function of total pressure and temperature. With $N_e(p, T)$ from line broadening a set of values p, T is found by graphical evaluation. The agreement with the values furnished by method α) was better than 10 %.

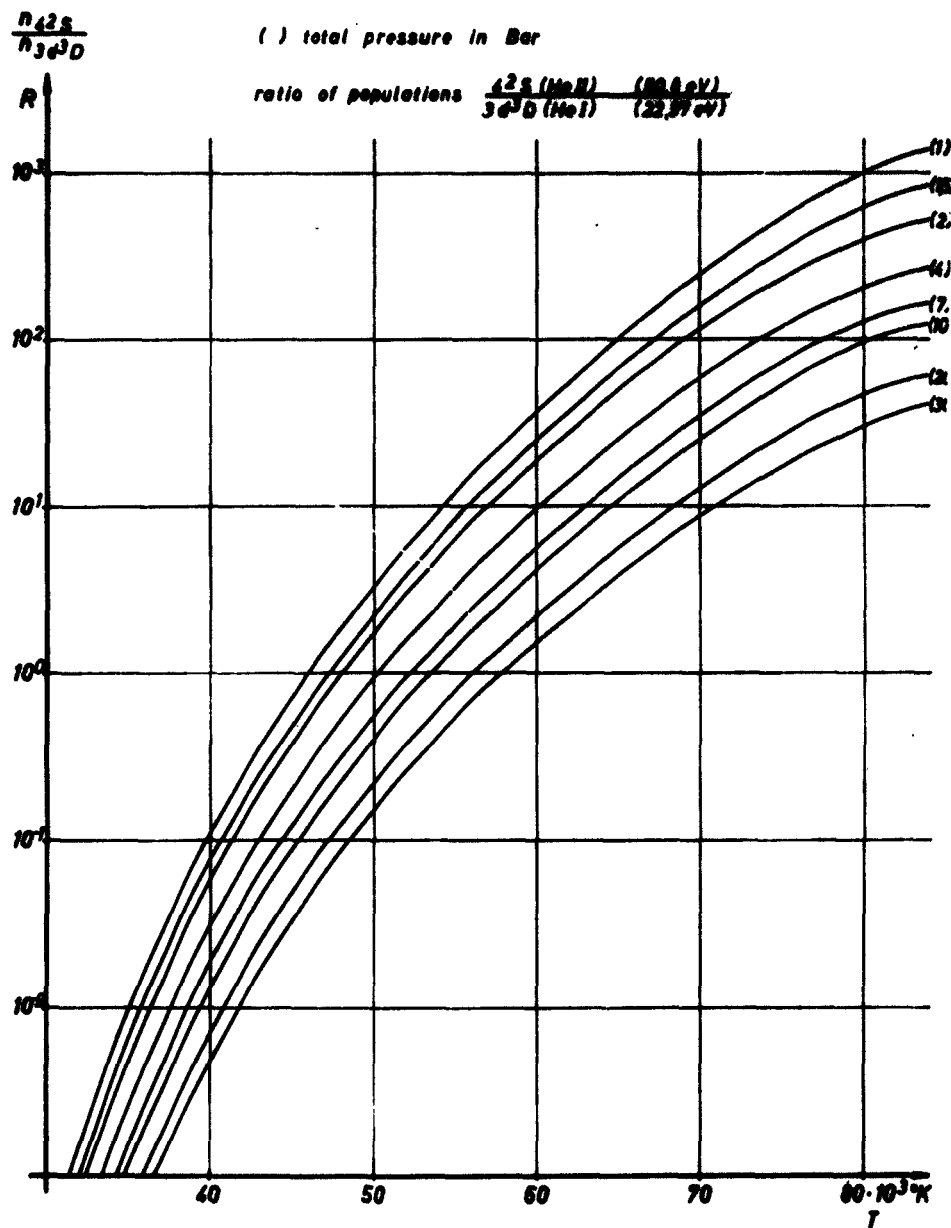


Fig. 24 . Ratio R of the populations of the upper states of the lines He II 4686 Å and He I 5876 Å.

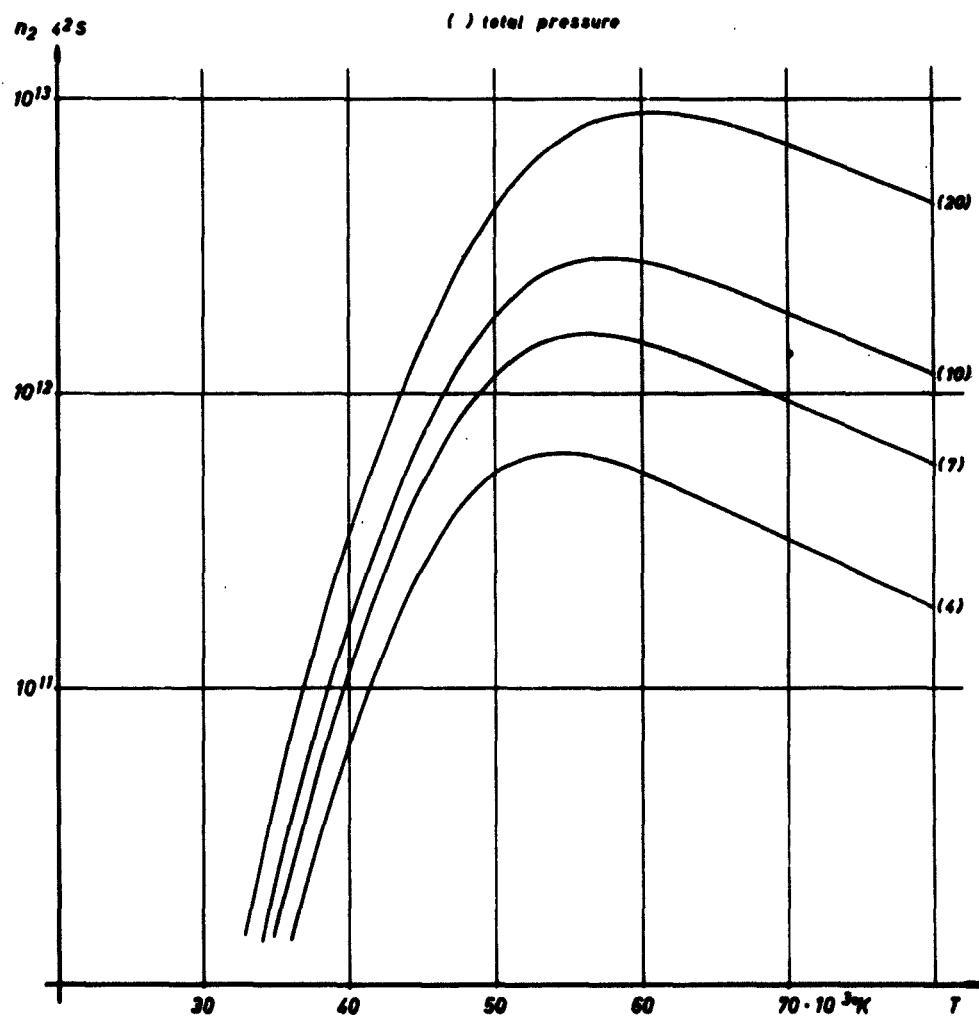


Fig. 25. Population of the upper state 4^2S of He II 4686 Å as a function of temperature and pressure.

γ) Temperature determination from the intensities of a neutral line and the continuum.

The ratio of the continuous intensity at 5220 \AA and of the line intensity of 5876 \AA is computed as a function of temperature and pressure and then plotted. These theoretical values (temperature and pressure were determined by method α) could be compared with the ratios obtained from the spectra. The agreement was within a factor 2.

Helium II lines or continuous background were not available at temperatures below 35000° K ; so the temperature and pressure must be determined only from helium I lines.

δ) Temperature determination from neutral line intensities.

From the measured absolute intensity of a neutral helium line the population of the upper level can be calculated using equations (5) and (6). Using the plot shown in fig. 26 and the electron density from the line width a set of values p, T is obtained.

2b) Plasma data in the magnetic compression experiment.

Using the methods described in the preceding chapter plasma parameters of the magnetically compressed discharge could be obtained as functions of time and space. The data resulting from the different quantitative spectroscopic measurements coincide quite well. This allows the conclusion that there is only small difference between excitation temperatures of the several species and on the other hand ionization temperatures. This justifies the assumption of local thermodynamic equilibrium in the plasma.

In fig. 27, 28, 29 the plasma parameters in the center of the discharge are plotted as functions of time. The time scale was determined from the different smear photographs.

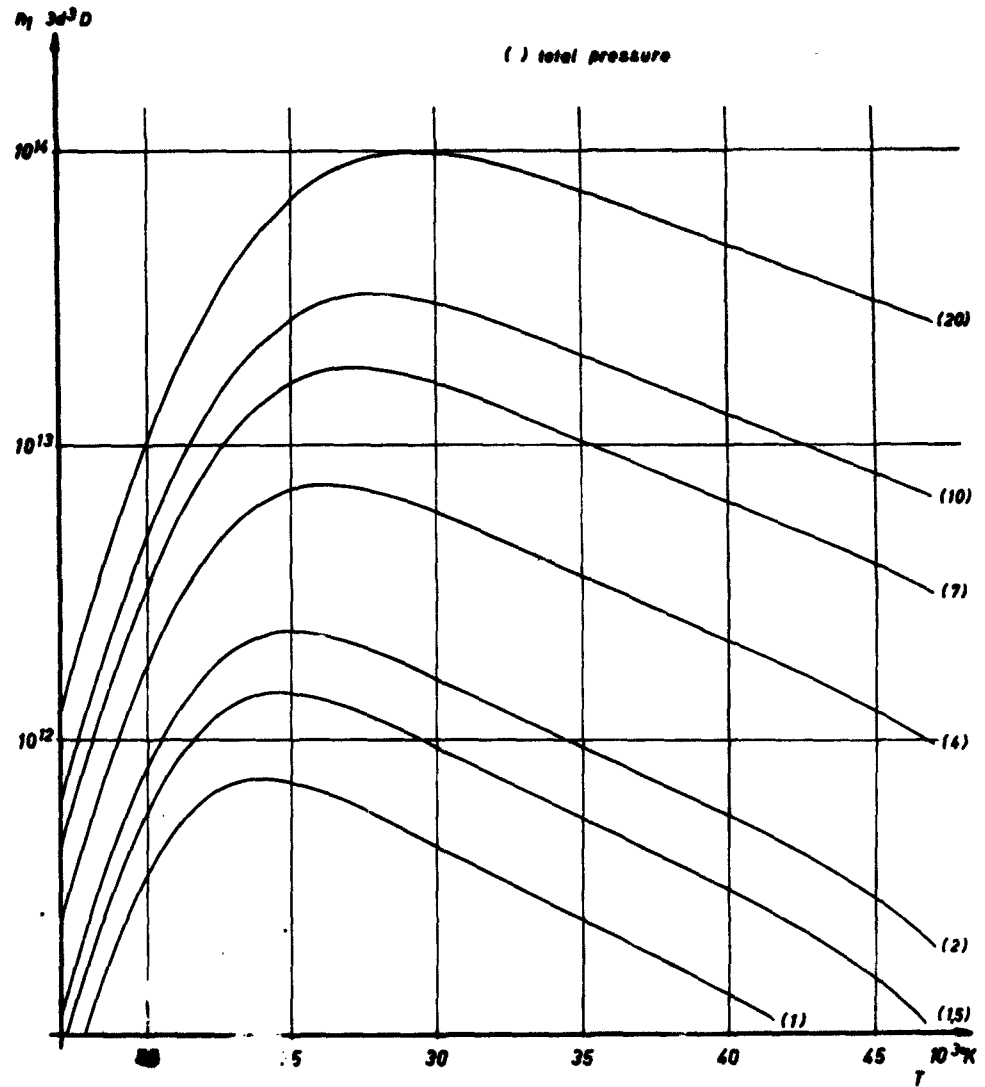


Fig. 26. The population of the upper level of He I 5876 Å $3d^3D$ as a function of pressure and temperature.

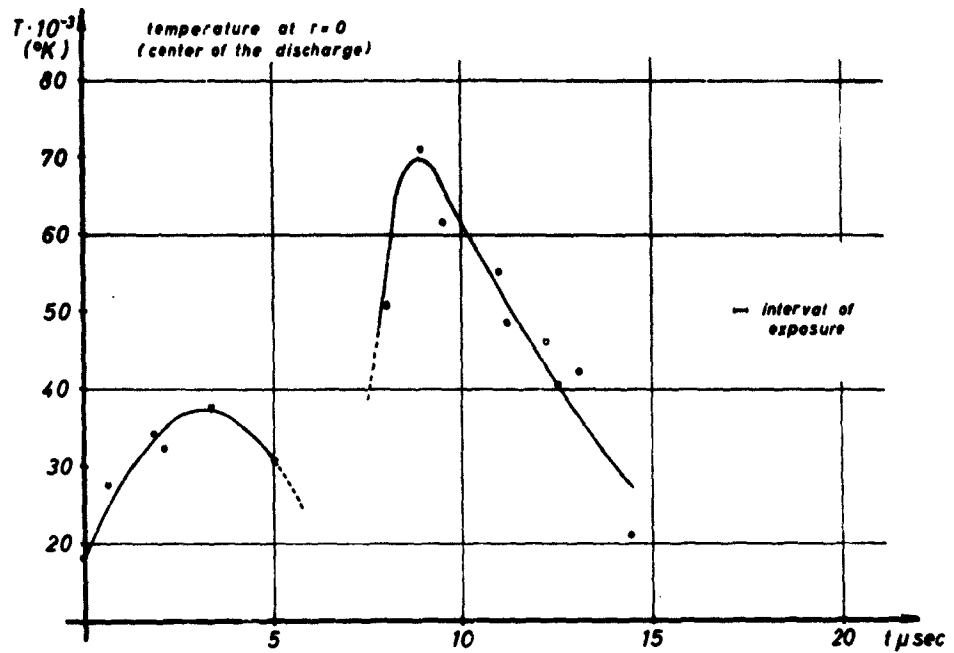


Fig. 27. The distribution of temperature in the center of the discharge as a function of time.

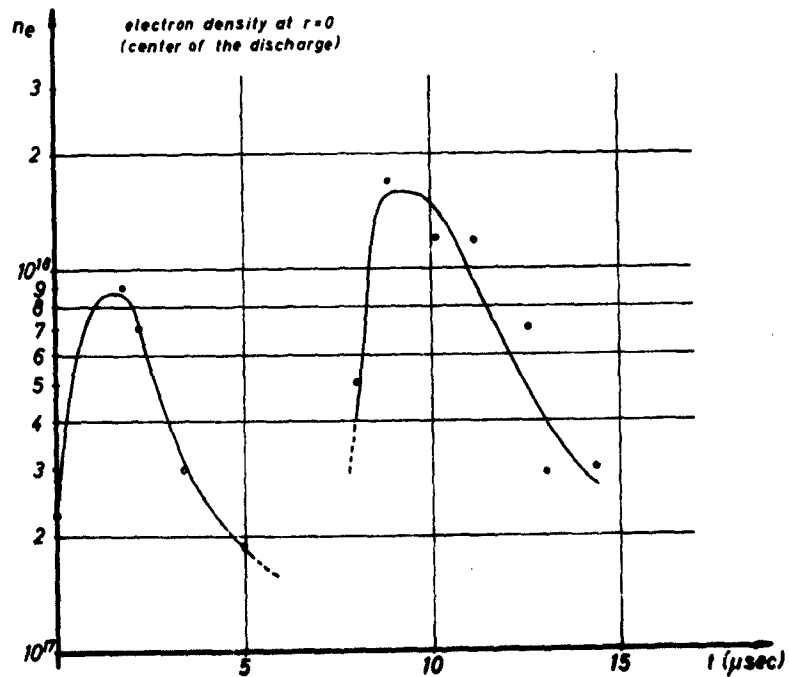


Fig. 28. The distribution of electron density in the center of the discharge as a function of time.

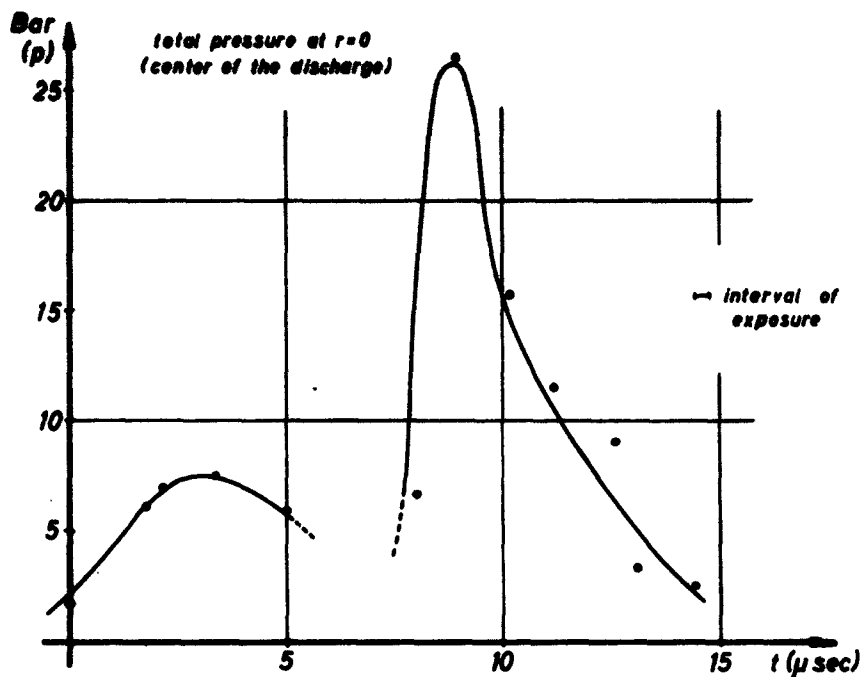


Fig. 29. Total pressure in the center of the discharge as a function of time.

From the spectra exposed in the different phases of the discharge the radial distribution of plasma parameters and its variation with time is obtained. Characteristic plots of the radial distribution are shown in fig. 30 and fig. 31.

Comparing the radial distributions at the different times mounts into the following result: in the second half-period the plasma radius (obtained from the p-, T- diagrams) rises with a velocity of about 10^6 cm sec^{-1} beginning at a value due to remaining preionization from the first half-period until temperature reaches its highest value. When temperature and pressure decrease the plasma more and more shaped as a hollow cylinder runs towards the wall of the discharge tube. Distinguished shock wave structure could not be observed.

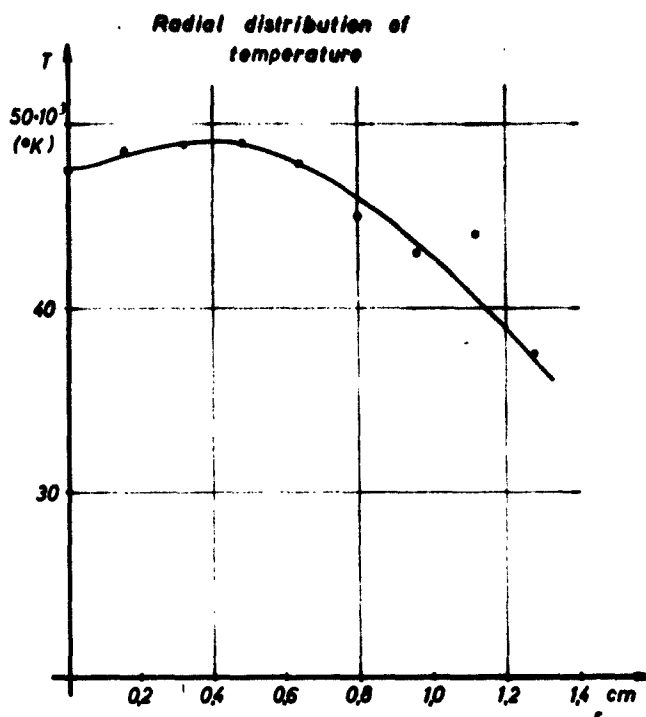


Fig. 30. Radial distribution of temperature in the magnetic compression experiment. The time of exposure is indicated in fig. 21 by arrows.

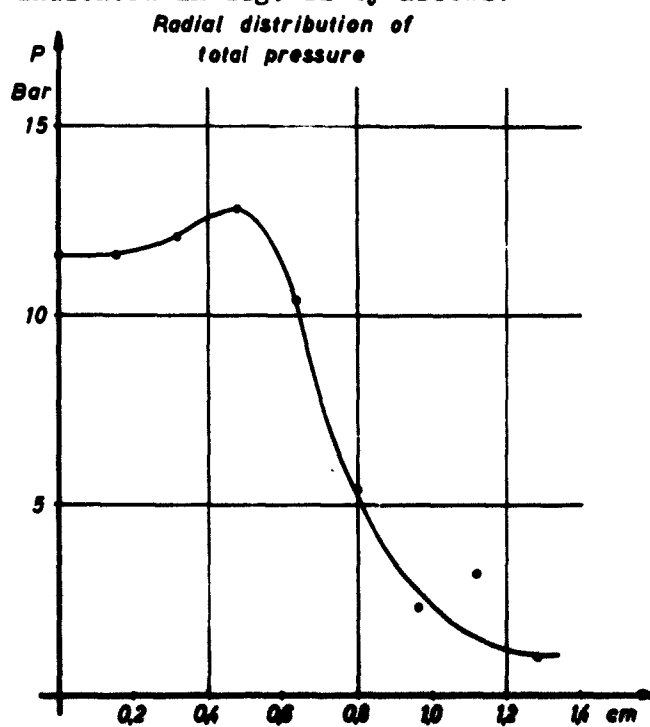


Fig. 31. Radial distribution of total pressure in the magnetic compression experiment. The time of exposure is indicated in fig. 21 by arrows.

E. Conclusion.

Magnetic compression of a discharge either by its own or by an outer magnetic field is the most promising procedure to produce plasmas at high temperatures. In the latter case the efficiency of heating is severely influenced by the degree of preionization. The use of a pulsed discharge of relatively high pressure in helium fed by a capacitor bank was very effective. Quantitative spectroscopic methods already proved in the range up to $30\,000^\circ\text{K}$ could be applied in plasma research up to $70\,000^\circ\text{K}$ at electron densities of more than 10^{18} cm^{-3} . In this way the evaluation of time resolved spectra yields plasma parameters being equal for the different methods used. This allows the conclusion that radiation is emitted from optically thin layers in local thermodynamic equilibrium and on the other hand proves the validity of spectroscopic formulae.

The temperatures reached may be further increased with more stored energy in the magnetic field capacitor bank and a more effective preionization. The study of magnetic compression modified in this way remains open to further investigation.

Bibliography

- 1) Jürgens, G., ZS. f. Phys. 134. 21. (1952)
Motschmann, H., ZS. f. Phys. 143. 77. (1955)
Bogen, P., ZS. f. Phys. 149. 62. (1957)
Maecker, H., ZS. Natf. 11a. 457. (1956)
Richter, J., ZS. f. Phys. 151. 114. (1958)
Wiese, W., Mastrup, F., ZS. f. Astrophys. 44. 259. (1958)
- 2) Maecker, H., Burhorn, Fr., ZS. f. Phys. 129. 369. (1951)
- 3) Wulff, H., ZS. f. Phys. 150. 614. (1958)
Christmann, H., Dipl.Arbeit, Kiel 1961 (unpublished)
Böttcher, W., Christmann, H., Fahrentholz, S.,
Kusch, H.J., Technical (final) Report Contract No.
AF 61(052)-368
- 4) Mahn, C., Dipl.Arbeit Kiel 1960, Tagung Bad Pyrmont 1960
Böttcher, W., V.International Conf. Ionisation
Phenomena in Gases, Munich 1961
- 5) Böttcher, W., Christmann, H., Fahrentholz, S.,
Kusch, H.J., Technical (Final) Report Contract
No. AF 61(052)-368
- 6) Hörmann, H., ZS. f. Phys. 97. 539. (1935)
Sperling, J., ZS. f. Phys. 128. 269. (1950)
- 7) Euler, J., Ann. Phys. 11. 203. (1953)
McPherson, H.G., Journ. Opt. Soc. Am. 30. 189. (1940)
- 8) Unsöld, A., ZS. f. Astrophys. 24. 355. (1948)
- 9) Unsöld, A., Physik der Sternatmosphären, Springer Berlin
2. Aufl. p. 166 (1955)
- 10) Kramers, H.A., Phil. Mag. 46. 836. (1923)
- 11) Griem, H.R., Baranger, M., Kolb, A.C., Oertel, G.,
Phys. Rev. 125. 177. (1962)
- 12) Shen, K.Y., Thesis Maryland Univ. 1960
Griem, H., Shen, K.Y., Phys. Rev. 122. 1490. (1961)
- 13) Berg, H.F., Thesis Maryland Univ. 1961
- 14) Sörensen, U., Richter, J., Kiel 1960 (unpublished)
- 15) Allen, C.W., Astrophysical Quantities, Athlone Press
London 1955 p. 67, 68

Glossary of symbols

a	Area of probing coil
A	Transition probability of a spectral line
B_v	Black body radiation function
c	velocity of light
C	Capacity
e	Elementary charge
g	statistical weight of an atomic energy level
H	Magnetic field strength
I	Light intensity
J	Current
κ_v	Absorption coefficient
l	length of light pointer
L	Inductivity
Λ	Logarithmic decrementum
m_e	Mass of electron
N_e	Electron density
ν	Frequency of a spectral line or of a rotating mirror
p	pressure
r	Radius vector
R_0	Radius of discharge tube
t	Time
T	Absolute temperatur
ω	Time of a full cycle of an oscillation
U, V	Voltage
w	Slit width
χ	Excitation potential
χ_v	Ionisation potential
x	Coordinate in space
Z	Ordinal number in the periodic system
Z_1	Partition function

List of illustrations

Fig.No.		Page
1	The connection of the capacitors (schematic)	4
2	Connection of the capacitors to the linear transmission line	5
3	Sparc gap of half-cylindrical shape	6
4	Total view of the pulse current condensor bank	7
5	Radial distribution of the magnetic field	8
6	Wiring of the triggering device switching the sparc gap	9
7	Diagram of the trigger circuit	9
8	Wiring of the capacitor bank used for preionization	10
9	Current of preionizing discharge	11
10	Photodiode triggering device	11
11	Wiring of the high-voltage supply for the preionizing glow discharge	12
12	Cross cut of the discharge tube	13
13	Optical arrangement for time resolved spectroscopy	14
14	Wiring of the photomultiplier triggering device	15
15	Circuit of the "Urtrigger"	16
16	The continuous emission of a helium plasma	20
17	The radial distribution of electron density in the preionizing discharge	22
18	The radial distribution of total pressure in the preionizing discharge	22
19	The radial distribution of temperature in the preionizing discharge	22
20	The spectrum of the preionizing discharge	23
21	Smear camera photograph of magnetic compression in helium	23
22	Characteristic spectrum of the first half-period of magnetic compression	24
23	Characteristic spectrum of the second half-period of magnetic compression	24
24	Ratio of the populations of the upper states of the lines He II 4686 Å and He I 5876 Å	26

Fig.No.		Page
25	Population of the upper state 4^2S of He II 4686 Å	27
26	The population of the upper level $3d^3D$ of He I 5876 Å	29
27	The distribution of temperature in the center of the discharge	30
28	The distribution of electron density in the center of the discharge	30
29	Total pressure in the center of the discharge	31
30	Radial distribution of temperature	32
31	Radial distribution of total pressure	32

Univ. of Kiel Contract:
Dept.: Inst. Exp. Phys. AF 61 ()
Lab. Rep. No. TN
Monitoring Agency: AD TR
Physics

DEVELOPMENT OF METHODS FOR QUANTITATIVE
SPECTROSCOPIC TEMPERATURE DETERMINATION
IN PLASMAS. Technical Final Report
Hans Jürgen Kusch, University of Kiel, Germany
June 30, 1962; 37 pages, 31 illustrations

The quick magnetic compression of a preionized
helium discharge was investigated. Plasma para-
meters were determined by several spectroscopic
methods using time resolution devices. Temperature
rises up to 70 000°K; electron density up to more
than 10¹⁸ cm⁻³.

USAF, European Office, ARDC, Brussels, Belgium

Univ. of Kiel Contract:
Dept.: Inst. Exp. Phys. AF 61 ()
Lab. Rep. No. TN
Monitoring Agency: AD TR
Physics

DEVELOPMENT OF METHODS FOR QUANTITATIVE
SPECTROSCOPIC TEMPERATURE DETERMINATION
IN PLASMAS. Technical Final Report
Hans Jürgen Kusch, University of Kiel, Germany
June 30, 1962; 37 pages, 31 illustrations

The quick magnetic compression of a preionized
helium discharge was investigated. Plasma para-
meters were determined by several spectroscopic
methods using time resolution devices. Temperature
rises up to 70 000°K; electron density up to more
than 10¹⁸ cm⁻³.

USAF, European Office, ARDC, Brussels, Belgium

Univ. of Kiel Contract:
Dept.: Inst. Exp. Phys. AF 61 ()
Lab. Rep. No. TN
Monitoring Agency: AD TR
Physics

DEVELOPMENT OF METHODS FOR QUANTITATIVE
SPECTROSCOPIC TEMPERATURE DETERMINATION
IN PLASMAS. Technical Final Report
Hans Jürgen Kusch, University of Kiel, Germany
June 30, 1962; 37 pages, 31 illustrations

The quick magnetic compression of a preionized
helium discharge was investigated. Plasma para-
meters were determined by several spectroscopic
methods using time resolution devices. Temperature
rises up to 70 000°K; electron density up to more
than 10¹⁸ cm⁻³.

USAF, European Office, ARDC, Brussels, Belgium

Univ. of Kiel Contract:
Dept.: Inst. Exp. Phys. AF 61 ()
Lab. Rep. No. TN
Monitoring Agency: AD TR
Physics

DEVELOPMENT OF METHODS FOR QUANTITATIVE
SPECTROSCOPIC TEMPERATURE DETERMINATION
IN PLASMAS. Technical Final Report
Hans Jürgen Kusch, University of Kiel, Germany
June 30, 1962; 37 pages, 31 illustrations

The quick magnetic compression of a preionized
helium discharge was investigated. Plasma para-
meters were determined by several spectroscopic
methods using time resolution devices. Temperature
rises up to 70 000°K; electron density up to more
than 10¹⁸ cm⁻³.

USAF, European Office, ARDC, Brussels, Belgium